

PropPy – Correlated random walk propagation of cosmic rays in magnetic turbulence

P. Reichherzer^{*1, 2, 3} and J. Becker Tjus^{1, 2}

¹ Ruhr-Universität Bochum, D-44801 Bochum, Germany ² Ruhr Astroparticle and Plasma Physics Center, D-44780 Bochum, Germany ³ Université Paris-Saclay, F-91190 Gif-sur-Yvette, France

DOI: [10.21105/joss.04153](https://doi.org/10.21105/joss.04153)

Software

- [Review](#) ↗
- [Repository](#) ↗
- [Archive](#) ↗

Editor: [Pending Editor](#) ↗

Submitted: 09 February 2022

Published: 10 February 2022

License

Authors of papers retain copyright and release the work under a Creative Commons Attribution 4.0 International License ([CC BY 4.0](#)).

Statement of need

Understanding the transport of charged high-energy particles (cosmic rays, CRs) in turbulent magnetic fields is essential for resolving the long-standing question of their extragalactic origin.

The transport properties of cosmic rays are relevant in many ways:

- In cosmic-ray sources, the transport properties determine their residence time in the sources and thus the interaction processes leading to the production of secondary particles ([Becker Tjus & Merten, 2020](#)).
- Due to the enormous distance from sources to our Galaxy, cosmic rays have to travel through the turbulent intergalactic medium ([Alves Batista et al., 2018](#)).
- In our Galaxy, the Galactic magnetic field influences their trajectory and, finally, their arrival in the Earth's atmosphere ([P. Reichherzer et al., 2022](#)).

Analytical theories have been developed over the last century ([Jokipii, 1966](#); [Schlickeiser, 2015](#); [Zweibel, 2013](#)) to describe the transport of cosmic rays. However, these theories are often limited by strongly simplifying assumptions concerning the transport of charged particles in turbulent magnetic fields. To overcome these limitations, propagation codes have been developed over the last decades to overcome these limitations with dedicated cosmic-ray-transport simulations (e.g., [Giagalone & Jokipii \(1999\)](#); [Casse et al. \(2001\)](#); [Shukurov et al. \(2017\)](#); [P. Reichherzer et al. \(2020\)](#); [P. Reichherzer, Becker Tjus, et al. \(2021\)](#)). In equation of motion (EOM) propagation methods, particles are moved stepwise, with the next step always determined based on the solution of the equation of motion with the external force as the Lorentz force only taking into account magnetic fields. Note the magnetic field must be computed for each propagation step for all particle positions, a process that is typically time-consuming in numerical simulations. This is especially relevant when the particles are highly diffusive, i.e., when the size of the propagation environment L exceeds the gyro radius of the particle $r_g \ll L$. A much more efficient method, the diffusive approach, is based on the statistical properties of the particles and exploits their theoretical description via a transport equation ([Merten et al., 2017](#)). In the limit of infinitely large times, diffusive transport occurs for all charged particles in isotropic turbulence. In the transport equation, the diffusion tensor implicitly contains all statistic properties. A major drawback of this approach is that can only model the transport of charged particles over large time scales so that the particles have enough time to become diffusive ([Becker Tjus et al., 2022](#)).

To tackle this issue and meet the need for realistic and fast simulations of the sources of cosmic rays, we present the software PropPy. Our software applies the approach of the correlated random walk (CRW), where statistical aspects are used for speed-up while also

^{*}first author

40 providing a good description of the initial phase. Additionally, the properties of the CRW can
41 be determined directly from the diffusion tensor and the gyration radius of the particle.

42 The comparison of the three different approaches diffusive, EOM, and CRW shows that CRW
43 simulation results are in good agreement with EOM simulations, while being considerably
44 faster.

45 Background Theory

46 First we assume particle transport in one dimension, where they can move either in positive
47 or negative direction along the x -axis. The following derivation has been discussed in various
48 contexts in the literature, such as when describing animal trails (see e.g. [Codling et al. \(2008\)](#)
49 for a review), and can also be applied for cosmic-ray propagation (see e.g., [Seta \(2019\)](#)).

50 During the CRW, the following two substeps are performed in each propagation step that
51 propagates particles for the time τ_s :

- 52 1. Particles that point in positive direction will turn around with the probability $\xi\tau_s$ and
53 otherwise continue along that direction with the probability $1 - \xi\tau_s$. The same applies
54 for particles that point in negative direction.
- 55 2. The particles move the distance χ with the speed $\chi/\tau_s \equiv v$ along the direction estab-
56 lished in the first substep.

57 If we divide the particle density per position at a given position x and time t into one dis-
58 tribution in positive direction $\alpha(x, t)$ and one in negative direction $\beta(x, t)$, the following sub-
59 distributions one propagation step later become

$$\alpha(x, t + \tau_s) = (1 - \xi\tau_s)\alpha(x - \chi, t) + \xi\tau_s\beta(x - \chi, t), \quad (1)$$

$$\beta(x, t + \tau_s) = \xi\tau_s\alpha(x + \chi, t) + (1 - \xi\tau_s)\beta(x + \chi, t). \quad (2)$$

61 As particles either move in positive or negative direction, the total particle distribution yields
62 $f(x, t) = \alpha(x, t) + \beta(x, t)$. Taylor expansion of a function $g(x, y)$ for two variables (x, y)
63 around (a, b) yields $g(x, y) = g(a, b) + \partial g/\partial x(a, b)(x - a) + \partial g/\partial y(a, b)(y - b) + \mathcal{O}(x^2, y^2)$.
64 Using this expansion for [Equation 1](#) and [Equation 2](#) for small steps $\tau_s, \chi \rightarrow 0$ around (x, t)
65 yields

$$\frac{\partial \alpha}{\partial t} = -v \frac{\partial \alpha}{\partial x} + \xi(\beta - \alpha), \quad (3)$$

$$\frac{\partial \beta}{\partial t} = v \frac{\partial \beta}{\partial x} - \xi(\beta - \alpha). \quad (4)$$

67 Here, we define $\alpha(x, t) \equiv \alpha$ and $\beta(x, t) \equiv \beta$ for simplicity. Adding component-wise [Equation 3](#)
68 and [Equation 4](#) yields

$$\frac{\partial(\alpha + \beta)}{\partial t} = v \frac{\partial(\beta - \alpha)}{\partial x}, \quad (5)$$

69 with the time derivative

$$\frac{\partial^2(\alpha + \beta)}{\partial t^2} = v \frac{\partial^2(\beta - \alpha)}{\partial t \partial x}. \quad (6)$$

70 Subtracting component-wise [Equation 3](#) from [Equation 4](#) and derivating with respect to x
71 yields

$$\frac{\partial^2(\beta - \alpha)}{\partial t \partial x} = v \frac{\partial^2(\alpha + \beta)}{\partial x^2} - 2\xi \frac{\partial(\beta - \alpha)}{\partial x}. \quad (7)$$

72 Inserting Equation 7 into Equation 6 results in

$$\frac{\partial^2(\alpha + \beta)}{\partial t^2} = v^2 \frac{\partial^2(\alpha + \beta)}{\partial x^2} - 2\xi v \frac{\partial(\beta - \alpha)}{\partial x}. \quad (8)$$

73 Inserting Equation 5 into Equation 8 yields

$$\frac{1}{2\xi} \frac{\partial^2(\alpha + \beta)}{\partial t^2} = \frac{v^2}{2\xi} \frac{\partial^2(\alpha + \beta)}{\partial x^2} - \frac{\partial(\alpha + \beta)}{\partial t}. \quad (9)$$

74 Finally, with $f = \alpha + \beta$, we have

$$\frac{1}{2\xi} \frac{\partial^2 f}{\partial t^2} = \frac{v^2}{2\xi} \frac{\partial^2 f}{\partial x^2} - \frac{\partial f}{\partial t}. \quad (10)$$

75 In fact, when we generalize this approach for three dimensions, assuming local homogeneity,
76 and connecting diffusion coefficients with the CRW parameters, this leads to the telegraph
77 equation

$$\frac{\partial f}{\partial t} + \sum_i \tau_i \frac{\partial^2 f}{\partial t^2} = \sum_i \kappa_i \frac{\partial^2 f}{\partial x_i^2}. \quad (11)$$

78 This verifies that the statistics of particles that follow CRW can be described with the telegraph
79 equation and thus agrees with analytical theories of particle transport of cosmic rays, see
80 previous work by e.g. Litvinenko et al. (2015); Tautz & Lerche (2016).

81 Comparison

82 In principle, the CRW propagation method implemented in PropPy can be applied wherever
83 other propagation codes for charged particles such as CRPropa (Alves Batista et al., 2016,
84 2021), DRAGON (Evoli et al., 2017), GALPROP (Strong & Moskalenko, 1998) are already
85 in use. However, the advantages of PropPy are especially in the high performance and the
86 accurate description of statistical transport properties also for the initial transport regime,
87 which is not possible for pure diffusive propagation approaches.

88 Charged particles (cosmic rays) are accelerated to high energies in astrophysical sources until
89 the gyration radius exceeds the system size according to the Hillas criterion, and the cos-
90 mic rays can no longer be confined by the accelerator. Since strong magnetic fields with a
91 significant amount of turbulence typically prevail in these sources, the description of particle
92 propagation in the sources is nontrivial and complicate the analytical description of transport.
93 As an example, we consider the transport of charged particles in AGN jets, an environment
94 for which the above codes are not optimized but whose underlying transport mechanisms can
95 still be applied.

96 Simulations are used for describing as accurately as possible the particle transport that has
97 an impact on numerous observable multimessenger signatures. In the following comparison,
98 we focus on the transport properties in these sources, which are described by the diffusion
99 coefficient.

100 Since CRPropa is the only code that supports both EOM and diffusive propagation methods
101 with anisotropic diffusion coefficients, this software (version: CRPropa 3.1.7) is used for
102 comparison simulations with PropPy.

103 While there are numerous possible sources covering a large parameter space of physical prop-
104 erties relevant to particle transport, for this comparison between PropPy propagation and
105 CRPropa modules, we use typical parameters used in the literature for AGN plasmoids (see,
106 e.g. Becker Tjus et al. (2022) and references therein):

- 107 ■ particle energies: $E = 100$ PeV

- 108 ■ isotropic 3d Kolmogorov turbulence
- 109 ■ magnetic field strength: $B_{\text{rms}} = 1 \text{ Gauss}$
- 110 ■ correlation length turbulence: $l_c \sim 10^{11} \text{ m}$

111 With these parameters, we can derive the expected diffusion coefficient from theory (Subedi
112 et al., 2017). These parameters result in gyroradii of the charged cosmic rays

$$r_g = \frac{\sqrt{2}E}{q c B} = \frac{141 \text{ PeV}}{q c \cdot 1\text{G}} \approx 4.72 \cdot 10^{12} \text{ m.} \quad (12)$$

113 Note that the factor $\sqrt{2}$ is introduced because of the isotropic directions of the magnetic field
114 vectors in the turbulence. Particles are in the quasi-ballistic transport regime ($r_g \gg l_c$), where
115 they experience only minor deflections. The expected diffusion coefficient κ is

$$\kappa_{\text{theory}} = \frac{r_g^2 \cdot c}{2l_c} = \frac{(4.72 \cdot 10^{12} \text{ m})^2 \cdot c}{2 \cdot 10^{11} \text{ m}} \approx 3.34 \cdot 10^{22} \frac{\text{m}^2}{\text{s}}. \quad (13)$$

116 This theoretical diffusion coefficient serves as an input for the diffusive and the CRW simula-
117 tions, and as a reference for all numerical simulations.

118 This diffusion coefficient results in expected mean-free paths of

$$\lambda_{\text{theory}} = \frac{3\kappa_{\text{theory}}}{c} \approx 3.34 \cdot 10^{14} \text{ m.} \quad (14)$$

119 Particles become diffusive at trajectory lengths of about λ , which is why the simulations are
120 stopped after trajectory lengths of 10^{17} m to have some buffer and a clear plateau in the
121 running diffusion coefficients.

122 As a simulation setting, 10^3 protons with $E = 100 \text{ PeV}$ are emitted isotropically from a
123 point source. The simulations and the presented results can be reproduced via the simulation
124 and analysis scripts provided in the comparison folder of PropPy 1.0.0 (Patrick Reichherzer,
125 2022b). The simulation results are available at (Patrick Reichherzer, 2022a).

126 The summation of planar waves with different wave numbers, amplitudes, and directions
127 generates the synthetic turbulence. Here, there are two possible approaches (Schlegel et al.,
128 2020):

- 129 1. The complete turbulence can be generated in advance of the simulation and stored on
130 a large grid by using an inverse discrete Fourier transform. During run-time, the local
131 magnetic field is computed via interpolation of the surrounding grid points that store
132 the magnetic field information. Here, the tri-linear interpolation is used as it is fast and
133 sufficiently accurate. The turbulence is stored on 1024^3 grid points.
- 134 2. As an alternative approach, the summation of different amplitudes, wavenumbers, and
135 directions can also be performed during run-time at the exact position where it is needed.
136 Numerous constraints of the first method, the grid method, are avoided in this plane-
137 wave (PW) approach, with the disadvantage that the simulations take longer. 1000
138 wave modes are used, which was determined to be sufficient in convergence tests.

139 Here, the performance of PropPy is compared to the two different propagation methods
140 implemented in CRPropa, which are:

- 141 1. Solving the EOM, using either the Boris-Push (BP) or the Cash-Karp (CK) algorithm.

142 2. Solving Stochastic Differential Equations (SDE). For this method, no turbulence has
143 to be generated, but only the diffusion coefficient has to be inputted, which already
144 contains the information on how the particles move statistically in the turbulence.

145 **Figure 1** shows a comparison of the simulation results for the calculated running diffusion
146 coefficients for the different methods of propagation and turbulence generation.

147 The left and right panels differ only in the simulation length. In the left panel, only trajectories
148 up to 10^{14} m are considered, whereas in the right panel, trajectories up to 10^{17} m are dis-
149 played. Since the mean-free path length indicates the transition between ballistic to diffusive
150 propagation, the left panel shows ballistic particle propagation and the right panel diffusive
151 propagation.

152 The top panel shows the running diffusion coefficients as a function of time. The middle panel
153 shows the effective diffusion coefficient at 10^{14} m on the left and the converged diffusion
154 coefficient on the right, since the running diffusion coefficient remains constant beginning at
155 the diffusive limit, as can be seen in the top panel.

156 The lowest panel shows the required processor time of the simulation as a function of the step
157 size. The same processor was used for all simulations for better comparability.

DRAFT

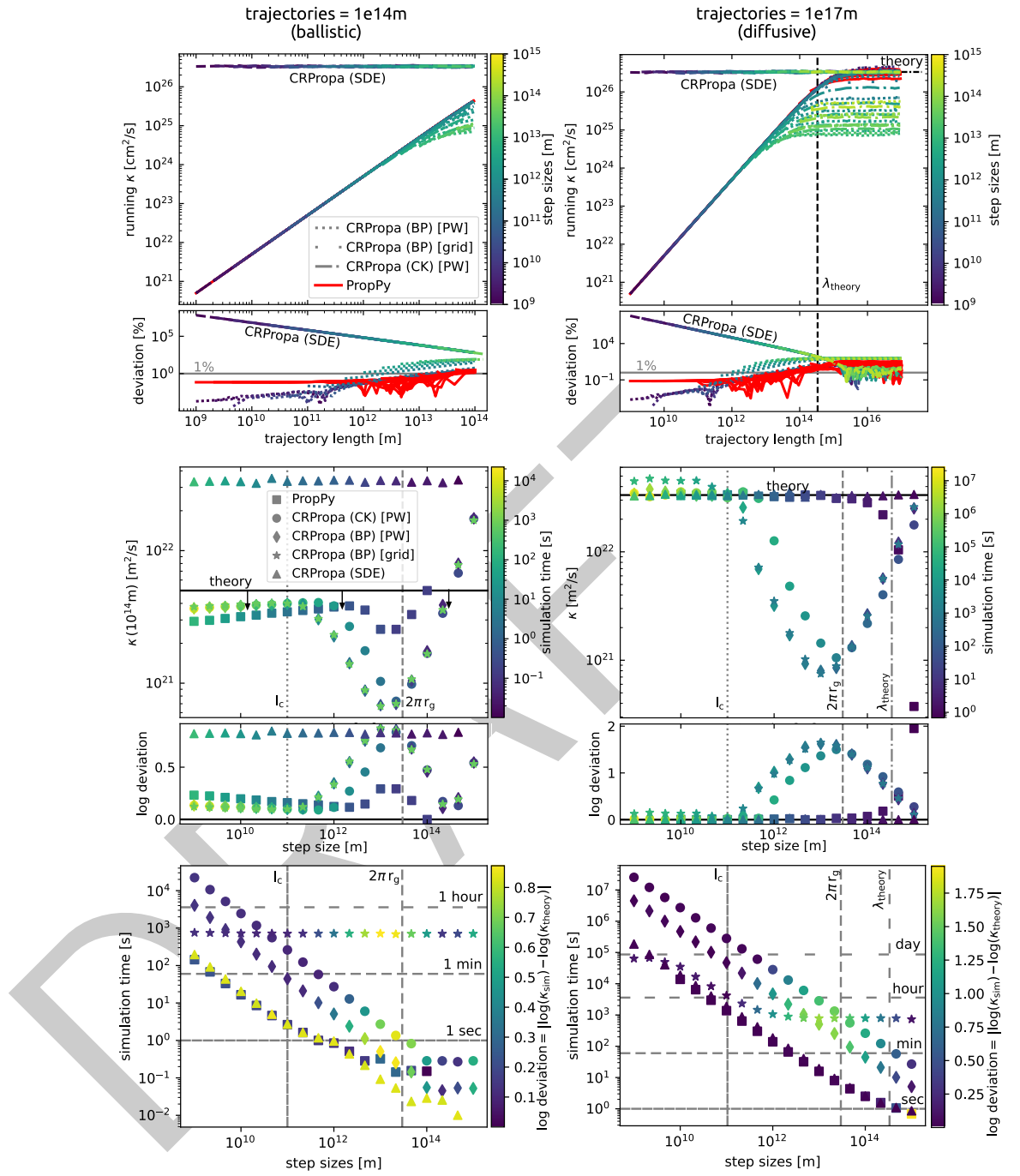


Figure 1: Comparison between different propagation approaches for the computation of running diffusion coefficients. 10^3 protons with $E = 10^{15}$ eV simulated in Kolmogorov turbulence generated with the grid and PW method described in the text. *Left panel* shows the ballistic propagation regime at the beginning of particle trajectories ($\leq 10^{14}$ m). *Right panel* shows also long trajectory lengths, for which the particle transport becomes diffusive ($\gg \lambda$). *Upper panel:* running diffusion coefficients as functions of trajectory lengths for different propagation methods. *Middle panel:* diffusion coefficients at 10^{14} m (left) and converged ones (right) as functions of different step sizes of the propagation methods. Log deviation is defined as $|\log(\kappa_{\text{sim}}) - \log(\kappa_{\text{theory}})|$. *Lower panel:* Simulation time per processor as functions of step sizes. Color-coded with the deviation from theoretical predictions. Usage of 260 threads for step sizes smaller than 10^{13} m. Note that the theory prediction is $\kappa_{\text{theo}} = 3.34 \cdot 10^{22} \text{ m}^2/\text{s}$. Averaging over 20 seeds of the same simulation with BP and PW with $s_{\text{step}} = 10^{10}$ m gives $\kappa_{\text{sim}} = (3.41 \pm 0.16) \cdot 10^{22} \text{ m}^2/\text{s}$.

158 The comparisons yield the following results:

- 159 ▪ The EOM-based propagation approaches BP and CK, as well as the CRW method from
160 PropPy can correctly model the initial ballistic transport phase. The diffusive approach
161 (SDE) can not describe this initial ballistic phase by construction since it always assumes
162 diffusive particle transport.
- 163 ▪ The diffusive approach and the CRW approach can use relatively large step sizes to
164 model the correct statistical behavior. The latter only needs to resolve the mean-free
165 paths sufficiently well, which is guaranteed if the step size at least ten times smaller than
166 the mean-free path. In the case of the EOM-based methods step sizes must be small
167 enough to resolve both the gyration motion and the scales of turbulence sufficiently
168 well. This can be seen as the diffusion coefficients in the middle right panel converge to
169 a constant value only when the step sizes are smaller than the gyration radii and smaller
170 than the correlation length of the turbulence.
- 171 ▪ Smaller simulation times for given step sizes in combination with the fewer step size
172 requirements translate into significant increase in speed for the diffusive method and
173 the CRW method compared to the EOM-based methods.

174 Conclusion

175 PropPy is an open-source python software for propagating charged high-energy particles in
176 a turbulent magnetic field. Its modular architecture comprises various modules for sources,
177 magnetic fields, propagators, and observers covering a wide range of applications.

178 When compared to codes that solve the EOM in each propagation step, our propagation is
179 based on a CRW in Cartesian (for isotropic diffusion) or cylindrical (for anisotropic diffusion)
180 coordinates, which makes each simulation step significantly faster. This novel approach is
181 justified by the fact that a transport equation can be derived via the formulation of the
182 CRW (see theory section below), which is used in analytical descriptions of particle transport
183 (Litvinenko et al., 2015; Tautz & Lerche, 2016):

$$\frac{\partial f}{\partial t} + \sum_i \tau_i \frac{\partial^2 f}{\partial t^2} = \sum_i \kappa_i \frac{\partial^2 f}{\partial x_i^2}, \quad (15)$$

184 where i indicates the three spatial directions, τ_i denotes the time scale for particles to become
185 diffusive, and κ_i is the diffusion coefficient, from which the relevant parameters of the CRW
186 can be determined.

187 Besides the analytical verification of the CRW ansatz, comparison simulations between PropPy
188 and an established cosmic-ray propagation software, CRPropa, are presented. These tests show
189 that both approaches are comparable in terms of the statistical properties such as the running
190 diffusion coefficient and the escape times from regions such as are relevant and present in
191 many astrophysical environments.

192 This makes PropPy a high-performance software for the simulation of charged particles in
193 turbulent magnetic fields. This is especially true for compact objects and transient events
194 with short time scales, such as gamma-ray bursts (GRBs), active galactic nuclei (AGN) flares,
195 where the accurate description of the initial particle propagation is crucial. Fast simulations
196 of transient events can help analyze observations and provide information to evaluate the
197 need for follow-up observations in the context of real-time multimessenger astrophysics (P.
198 Reichherzer, Schüssler, et al., 2021).

Acknowledgements

We acknowledge support from funding from the German Science Foundation DFG, within the Collaborative Research Center SFB1491 “Cosmic Interacting Matters - From Source to Signal.” Special thanks to L. Schlegel, F. Schüssler, J. Suc, and E.G. Zweibel for valuable discussions.

References

- Alves Batista, R., Becker Tjus, J., Dörner, J., Dundovic, A., Eichmann, B., Frie, A., Heiter, C., Hoerbe, M., Kampert, K., Merten, L., Müller, G., Reichherzer, P., Saveliev, A., Schlegel, L., Sigl, G., Vliet, A. van, & Winchen, T. (2021). CRPropa 3.2: a framework for high-energy astroparticle propagation. *arXiv e-Prints*, arXiv:2107.01631. <https://doi.org/10.22323/1.395.0978>
- Alves Batista, R., de Gouveia Dal Pino, E. M., Dolag, K., & Hussain, S. (2018). Cosmic-ray propagation in the turbulent intergalactic medium. *arXiv e-Prints*, arXiv:1811.03062. <http://arxiv.org/abs/1811.03062>
- Alves Batista, R., Dundovic, A., Erdmann, M., Kampert, K.-H., Kuempel, D., Müller, G., Sigl, G., Vliet, A. van, Walz, D., & Winchen, T. (2016). CRPropa 3a public astrophysical simulation framework for propagating extraterrestrial ultra-high energy particles. *JCAP*, 2016(5), 038. <https://doi.org/10.1088/1475-7516/2016/05/038>
- Becker Tjus, J., Hörbe, M., Jaroschewski, I., Reichherzer, P., Rhode, W., Schroller, M., & Schüssler, F. (2022). Propagation of cosmic rays in plasmoids of AGN jets – implications for multimessenger predictions. *arXiv e-Prints*, arXiv:2202.01818. <http://arxiv.org/abs/2202.01818>
- Becker Tjus, J., & Merten, L. (2020). Closing in on the origin of Galactic cosmic rays using multimessenger information. *Physrep*, 872, 1–98. <https://doi.org/10.1016/j.physrep.2020.05.002>
- Casse, F., Lemoine, M., & Pelletier, G. (2001). Transport of cosmic rays in chaotic magnetic fields. *PRD*, 65(2), 023002. <https://doi.org/10.1103/PhysRevD.65.023002>
- Codling, E. A., Plank, M. J., & Benhamou, S. (2008). Random walk models in biology. *Journal of The Royal Society Interface*, 5(25), 813–834. <https://doi.org/10.1098/rsif.2008.0014>
- Evoli, C., Gaggero, D., Vittino, A., Di Bernardo, G., Di Mauro, M., Ligorini, A., Ullio, P., & Grasso, D. (2017). Cosmic-ray propagation with DRAGON2: I. numerical solver and astrophysical ingredients. *JCAP*, 2017(2), 015. <https://doi.org/10.1088/1475-7516/2017/02/015>
- Giagalone, J., & Jokipii, J. R. (1999). The Transport of Cosmic Rays across a Turbulent Magnetic Field. *AjJ*, 520(1), 204–214. <https://doi.org/10.1086/307452>
- Hoerbe, M. R., Morris, P. J., Cotter, G., & Becker Tjus, J. (2020). On the relative importance of hadronic emission processes along the jet axis of active galactic nuclei. 496(3), 2885–2901. <https://doi.org/10.1093/mnras/staa1650>
- Jokipii, J. R. (1966). Cosmic-Ray Propagation. I. Charged Particles in a Random Magnetic Field. *ApJ*, 146, 480. <https://doi.org/10.1086/148912>
- Litvinenko, Y. E., Effenberger, F., & Schlickeiser, R. (2015). The Telegraph Approximation for Focused Cosmic-Ray Transport in the Presence of Boundaries. *ApJ*, 806(2), 217. <https://doi.org/10.1088/0004-637X/806/2/217>

- 243 Merten, L., Becker Tjus, J., Fichtner, H., Eichmann, B., & Sigl, G. (2017). CRPropa 3.1a
244 low energy extension based on stochastic differential equations. *JCAP*, 2017(6), 046.
245 <https://doi.org/10.1088/1475-7516/2017/06/046>
- 246 Reichherzer, Patrick. (2022a). *Comparison of propagation tools CRPropa and PropPy* [Data
247 set]. Zenodo. <https://doi.org/10.5281/zenodo.5959618>
- 248 Reichherzer, Patrick. (2022b). *Correlated random walk propagation of cosmic rays in mag-*
249 *netic turbulence* (Version v1.0.0) [Computer software]. Zenodo. [https://doi.org/10.5281/](https://doi.org/10.5281/zenodo.5959220)
250 [zenodo.5959220](https://doi.org/10.5281/zenodo.5959220)
- 251 Reichherzer, P., Becker Tjus, J., Zweibel, E. G., Merten, L., & Pueschel, M. J. (2020).
252 Turbulence-level dependence of cosmic ray parallel diffusion. *MNRAS*, 498(4), 5051–5064.
253 <https://doi.org/10.1093/mnras/staa2533>
- 254 Reichherzer, P., Becker Tjus, J., Zweibel, E. G., Merten, L., & Pueschel, M. J. (2021).
255 Anisotropic cosmic-ray diffusion in isotropic Kolmogorov turbulence. *arXiv e-Prints*,
256 arXiv:2112.11827. <http://arxiv.org/abs/2112.11827>
- 257 Reichherzer, P., Merten, L., & Dörner et al., J. (2022). Regimes of cosmic-ray diffusion in
258 Galactic turbulence. *arXiv e-Prints*, 4(15). <https://doi.org/10.1007/s42452-021-04891-z>
- 259 Reichherzer, P., Schüssler, F., Lefranc, V., Yusafzai, A., Alkan, A. K., Ashkar, H., & Becker
260 Tjus, J. (2021). Astro-COLIBRI-The COincidence LIBrary for Real-time Inquiry for Mul-
261 timessenger Astrophysics. *ApJS*, 256(1), 5. <https://doi.org/10.3847/1538-4365/ac1517>
- 262 Schlegel, L., Frie, A., Eichmann, B., Reichherzer, P., & Becker Tjus, J. (2020). Interpolation
263 of Turbulent Magnetic Fields and Its Consequences on Cosmic Ray Propagation. *APJ*,
264 889(2), 123. <https://doi.org/10.3847/1538-4357/ab643b>
- 265 Schlickeiser, R. (2015). Cosmic ray transport in astrophysical plasmas. *Physics of Plasmas*,
266 22(9), 091502. <https://doi.org/10.1063/1.4928940>
- 267 Seta, A. (2019). *Cosmic ray propagation in turbulent galactic magnetic fields*.
- 268 Shukurov, A., Snodin, A. P., Seta, A., Bushby, P. J., & Wood, T. S. (2017). Cosmic Rays in
269 Intermittent Magnetic Fields. *ApJL*, 839(1), L16. [https://doi.org/10.3847/2041-8213/](https://doi.org/10.3847/2041-8213/aa6aa6)
270 [aa6aa6](https://doi.org/10.3847/2041-8213/aa6aa6)
- 271 Strong, A. W., & Moskalenko, I. V. (1998). Propagation of Cosmic-Ray Nucleons in the
272 Galaxy. *ApJ*, 509(1), 212–228. <https://doi.org/10.1086/306470>
- 273 Subedi, P., Sonsrtee, W., Blasi, P., Ruffolo, D., Matthaeus, W. H., Montgomery, D., Chuy-
274 chai, P., Dmitruk, P., Wan, M., Parashar, T. N., & Chhiber, R. (2017). Charged Particle
275 Diffusion in Isotropic Random Magnetic Fields. 837(2), 140. [https://doi.org/10.3847/](https://doi.org/10.3847/1538-4357/aa603a)
276 [1538-4357/aa603a](https://doi.org/10.3847/1538-4357/aa603a)
- 277 Tautz, R. C., & Lerche, I. (2016). Application of the three-dimensional telegraph equation
278 to cosmic-ray transport. *Research in Astronomy and Astrophysics*, 16(10), 162. <https://doi.org/10.1088/1674-4527/16/10/162>
- 280 Zweibel, E. G. (2013). The microphysics and macrophysics of cosmic rays. *Physics of Plasmas*,
281 20(5), 055501. <https://doi.org/10.1063/1.4807033>